ELSEVIER

International Journal of Refrigeration 23 (2000) 197–207

REVUE INTERNATIONALE DU FROID
INTERNATIONAL JOURNAL OF
refrigeration

www.elsevier.com/locate/ijrefrig

System dynamic model and temperature control of a thermoelectric cooler

B.J. Huang*, C.L. Duang

Department of Mechanical Engineering, National Taiwan University, Taipei, Taiwan

Received 2 June 1998; received in revised form 15 April 1999; accepted 18 August 1999

Abstract

A linear dynamic model of the thermoelectric cooler including the heat sink and the cooling-load heat exchanger was derived using small-signal linearization method. It shows that the dynamic model of a thermoelectric cooler has two poles and one zero. The linear dynamic model is shown to vary with operating conditions. A linear feedback system is designed for the cold-end temperature control of a thermoelectric cooler using the average linear dynamic model of the thermoelectric cooler and a PDF controller structure. The step response tests show that the controller has a very satisfactory performance. Some tests under variable cooling load and ambient temperature are also performed to examine the disturbance-rejection property of the controller. Experimental results show that the cold-end temperature can be maintained at the fixed value within ± 0.1°C irrespective of the variations of the cooling load and the ambient conditions.

Keywords: Refrigerating system; Thermoelectricity; Operating; Simulation; Measurement; Accuracy

Modèle dynamique d'un système et régulation de la température d'un refroidisseur thermoélectrique

Résumé

Un modèle dynamique linéaire d'un refroidisseur thermoélectrique, y compris du puits thermique et de l'échangeur froid a été conçu à l'aide d'une méthode de linéarisation des signaux de basse intensité. Les auteurs montrent que le modèle dynamique d'un refroidisseur thermoélectrique possède deux pôles et une valeur zéro. On a vu que le modèle dynamique linéaire varie selon les conditions de fonctionnement.

Un système de rétroaction linéaire est conçu pour assurer la régulation de la température côté froid d'un refroidisseur thermoélectrique à l'aide du modèle dynamique linéaire et une régulation PDF. Les essais sur la réponse par paliers ont montré que la performance du régulateur est très satisfaisante. Les essais effectués dans diverses conditions de charge frigorifique et de température ambiante ont permis d'examiner les propriétés de perturbation/rejet du régulateur. Les résultats experimentaux ont montré que la température côté froid peut être maintenue à une valeur fixée avec une précision de ± 0,1 °C, quelques soient les variations de la charge frigorifique et les conditions ambiantes.

Mots clés: Système frigorifique; Thermoélectricité; Fonctionnement; Simulation; Mesure; Précision

* Corresponding author. Tel.: +886-2-2363-4790; fax: +886-2-2364-0549.
E-mail address: bjhuang@tpts6.seed.net.tw (B.J. Huang).

0140-7007/00/$20.00
PII: S0140-7007(99)00045-6

Nomenclature

A	total cross-sectional area of the thermoelectric material (m^2)
A_F	total heat transfer surface area of the heat sink (m^2)
A_p	gain of the power amplifier (actuator) ($A\ V^{-1}$)
C	mean heat capacity of the thermoelectric module ($kJ\ kg^{-1}\ K^{-1}$)
C_c	heat capacity of the cold-end plate of thermoelectric module ($kJ\ kg^{-1}\ K^{-1}$)
C_F	heat capacity of heat sink ($kJ\ kg^{-1}\ K^{-1}$)
C_H	heat capacity of the hot-end plate of thermoelectric module ($kJ\ kg^{-1}\ K^{-1}$)
C_L	heat capacity of the cooling-load heat exchanger ($kJ\ kg^{-1}\ K^{-1}$)
$G_I(s)$	transfer-function model of the thermoelectric cooler defined in Eq. (21)
h	convective heat transfer coefficient of the heat sink ($W\ m^{-2}\ K^{-1}$)
I	applied current to the thermoelectric module (A)
k	mean thermal conductivity of the thermoelectric p–n pair ($W\ m^{-1}\ K^{-1}$)
K	gain of the dynamic model of thermoelectric cooler defined in Eq. (23)
K_I	integral control parameter
K_g	gain of the measurement instrument ($V\ K^{-1}$)
K_p	controller gain
L	length of the thermoelectric elements (m)
M_c	mass of the cold-end plate of thermoelectric module
M_F	mass of the heat sink
M_H	mass of the hot-end plate of thermoelectric module
M_L	mass of the cooling-load heat exchanger
p	a transfer-function relation defined in Eq. (17)
p_1,p_2	poles of the dynamic model of the thermoelectric cooler defined in Eq. (23)
q	a transfer-function relation defined in Eq. (17)
Q_k	heat conduction of the thermoelectric material at the cold end (W)
Q_L	cooling load of the thermoelectric cooler (W)
Q_o	heat conduction of the thermoelectric material at the hot end (W)
s	complex variable
T	temperature distribution in the thermoelectric material (K)
T_a	ambient temperature (K)
T_H	temperature of the hot side of the thermoelectric module (K)
T_L	temperature of the cold side of the thermoelectric module (K)
x	position in the thermoelectric leg measured from the cold side (m)
z	zero of the dynamic model of the thermoelectric cooler defined in Eq. (23)

Greek letters

α_{pn}	Seeback coefficient of thermoelectric material ($V\ K^{-1}$)
ρ	mean electrical resistance of the thermoelectric material ($\Omega - m$)
γ	mean density of the thermoelectric material ($kg\ m^{-3}$)
τ	Thomson coefficient ($V\ K^{-1}$)

Superscripts

$^-$	mean; steady state; average
$^\sim$	perturbation; small signal

1. Introduction

Thermoelectric cooler has been frequently used for the cooling of electronic devices such as CPU, infrared sensor, ice-point reference in thermocouple thermometry, and refrigerators [1–3]. Usually, the temperature at the cold side of the thermoelectric module where an electronic part such as infrared sensor is mounted needs to be maintained at a constant and stable value under variable hot-side and ambient temperatures. This relies on a good temperature control technique.

For a better controller design, we have to know the system dynamic model of the thermoelectric cooler first. Many researchers studied the dynamic or transient behavior of thermoelectric element [4–7]. Using small-signal linearization method, Gray [4] theoretically derived a transfer-function model to calculate the temperature response of a thermoelectric element. Bywaters and Blum [6] assumed that the temperature distribution in the thermoelectric elements is linear and solved the governing equations. These studies [4–7] are basically for the analysis of a pair of thermoelectric elements.

For a thermoelectric module that consists of many pairs of thermoelectric elements, the theoretical analysis may cause some errors. In addition, the ignorance of the effect of thermal masses connected at the cold and hot sides of a thermoelectric module will cause significant error in the temperature control. In the present study, we have carried out a testing to determine the system dynamic model of a thermoelectric cooler (including the module and the thermal masses of heat sink and cooling-load heat exchanger) using the system identification

technique. The structure of the dynamic model is determined first from a theoretical derivation using the method of small-signal linearisation. The parameters of the dynamic model are experimentally identified at various operating conditions. The average model is used in the design of a control system for the cold-end temperature control of the thermoelectric cooler.

2. System dynamic model of a thermoelectric cooler

2.1. Governing equations

A thermoelectric cooler consists of a thermoelectric module, a heat sink connected to the hot side, and a cooling-load heat exchanger connected to the cold side. The thermoelectric module comprises many pairs of *p–n* type thermoelectric material connected in series and clamped and soldered with two base plates (e.g. aluminum oxide) (see Fig. 1). The heat load Q_L is absorbed at the cooling-load heat exchanger, conducted to the hot-end plate, and then pumped to the hot side of the thermoelectric module.

Assume that the temperature distributions inside the cold-end plate and the cooling-load heat exchanger are uniform. Energy balance to the cold-end plate and the cooling-load heat exchanger as a whole leads to

$$(M_L C_L + M_c C_c)\frac{\mathrm{d}T_L}{\mathrm{d}t} = Q_L - Q_k - I\alpha_{pn}T_L \tag{1}$$

where Q_k is the heat conduction at the cold-end boundary of the thermoelectric module which is expressed as

$$Q_k = -kA\left.\frac{\partial T(x,t)}{\partial x}\right|_{x=0} \tag{2}$$

where k is the mean thermal conductivity of the *p–n* material; A is the total cross-sectional area of the thermoelectric material; $T(x, t)$ is the temperature distribution of the thermoelectric module.

Energy balance to the thermoelectric material will lead to the relation:

$$C\gamma\frac{\partial T(x,t)}{\partial t} = k\frac{\partial^2 T(x,t)}{\partial x^2} - \frac{\tau}{A}I\frac{\partial T(x,t)}{\partial x} + \frac{\rho}{A^2}I^2 \tag{3}$$

where τ is the Thomson coefficient defined as $T\mathrm{d}\alpha_{pn}/\mathrm{d}T$; ρ is the mean electrical resistance of the thermoelectric material; C is the mean specific heat of the thermoelectric material; γ is the mean density of the thermoelectric material. The second term on the right hand side of Eq. (3) represents the heat resulting from Thomson effect [6,8].

Similarly, energy balance to the heat sink and the hot-side plate as a whole leads to

$$(M_F C_F + M_H C_H)\frac{\mathrm{d}T_H}{\mathrm{d}t} = I\alpha_{pn}T_H + Q_o - hA_F(T_H - T_a) \tag{4}$$

where Q_o is the heat conduction at the hot-side boundary of the thermoelectric module which can be expressed as

$$Q_o = -kA\left.\frac{\partial T}{\partial x}\right|_{x=L} \tag{5}$$

Eqs. (1), (3) and (4) are the governing equations for the dynamic behavior of a thermoelectric cooler. The model is highly nonlinear due to the temperature dependence of physical properties, the resistive heat, and the Peltier effect. Linearization using small-signal analysis is necessary since the controller design will be based on linear system theory.

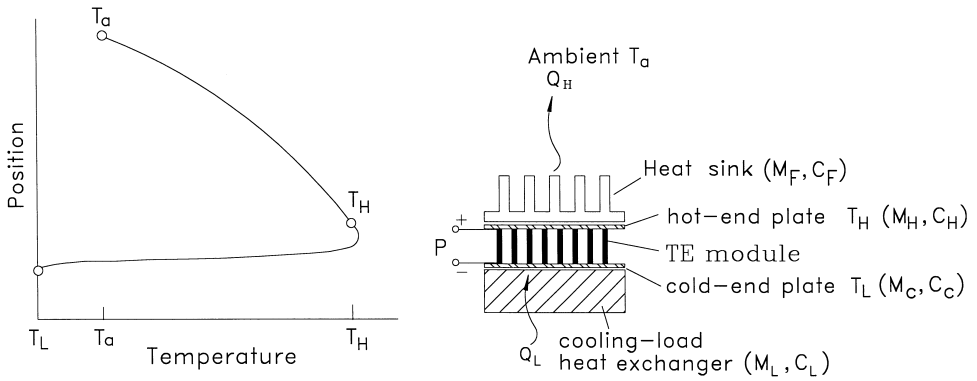

Fig. 1. Schematic diagram of thermoelectric and temperature distribution.

Fig. 1. Schéma de la distribution thermoélectrique et de température.

2.2. Linearization

Let all the variables of the thermoelectric cooler be the summation of a steady-state value and a perturbed quantity, i.e.

$$\begin{aligned} &T(x,t)=\bar{T}(x)+\tilde{T}(x,t); \quad && T_L(t)=\bar{T}_L+\tilde{T}_L(t);\\ &T_H(t)=\bar{T}_H+\tilde{T}_H(t); && T_a(t)=\bar{T}_a+\tilde{T}_a(t);\\ &Q_L(t)=\bar{Q}_L+\tilde{Q}(t); && I(t)=\bar{I}+\tilde{I}(t), \end{aligned} \tag{6}$$

and use the approximate relation of the Seeback coefficient according to Taylor's series expansion:

$$\alpha_{pn}(T)=\alpha_L+\frac{\tau}{\bar{T}_L}\tilde{T}_L=\alpha_H+\frac{\tau}{\bar{T}_H}\tilde{T}_H \tag{7}$$

where $\alpha_L=\alpha_{pn}(\bar{T}_L)$; $\alpha_H=\alpha_{pn}(\bar{T}_H)$. Substituting Eqs.(6) and (7) into Eqs. (1), (3) and (4), ignoring the high order terms, and eliminating the steady-state terms, we obtain, for constant properties τ, k, ρ, C, γ,

$$k\frac{\partial^2\tilde{T}}{\partial x^2}-\frac{\tau\bar{I}}{A}\frac{\partial\tilde{T}}{\partial x}+\left[\frac{2\rho\bar{I}}{A^2}-\frac{\tau(\bar{T}_H-\bar{T}_L)}{AL}\right]\tilde{I}=C\gamma\frac{\partial\tilde{T}}{\partial t} \tag{8}$$

$$\begin{aligned} &\tilde{Q}_L-(\alpha_L+\tau)\bar{I}\tilde{T}_L-\alpha_L\bar{T}_L\tilde{I}+kA\left.\frac{\partial\tilde{T}}{\partial x}\right|_{x=0}\\ &\quad=(M_LC_L+M_cC_c)\frac{\mathrm{d}\tilde{T}_L}{\mathrm{d}t} \end{aligned} \tag{9}$$

$$\begin{aligned} &(\alpha_H+\tau)\bar{I}\tilde{T}_H+\alpha_H\bar{T}_H\tilde{I}-kA\left.\frac{\partial\tilde{T}}{\partial x}\right|_{x=L}-hA_F(\tilde{T}_H-\tilde{T}_a)\\ &\quad=(M_FC_F+M_HC_H)\frac{\mathrm{d}\tilde{T}_H}{\mathrm{d}t} \end{aligned} \tag{10}$$

Eq. (8) is obtained from an assumption that the steady-state temperature distribution in the thermoelectric material is linear, i.e.$\mathrm{d}\bar{T}(x)/\mathrm{d}x\approx(\bar{T}_H-\bar{T}_L)/L$.

2.3. System dynamic model of thermoelectric cooler

Solving Eqs, (8)–(10) by Laplace transform, we obtain the transfer function of the perturbed cold-end temperature:

$$\tilde{T}_L(s)=G_I(s)\tilde{I}(s)+G_Q(s)\tilde{Q}_L(s)+G_a(s)\tilde{T}_a(s) \tag{11}$$

where

$$G_I(s)=\frac{N(s)}{sD(s)} \tag{12}$$

$$G_Q(s)=\frac{E_H\sinh(qL)+Akq\cosh(qL)}{D(s)} \tag{13}$$

$$G_a(s)=\frac{AA_Fhkq}{D(s)} \tag{14}$$

where

$$\begin{aligned} N(s)=&\Big\{Akq[\alpha_L\bar{T}_L\cosh(qL)-\alpha_H\bar{T}_H]\\ &+\alpha_L\bar{T}_LE_H\sinh(qL)\Big\}s\\ &+\frac{Akq\beta}{C\gamma}[E_H(1-\cosh pL)-Akp\sinh pL] \end{aligned} \tag{15}$$

$$\begin{aligned} D(s)=&AkqE_L\cosh(qL)+E_HE_L\sinh(qL)\\ &+AkqE_H\cosh(pL)+A^2k^2pq\sinh(pL) \end{aligned} \tag{16}$$

$$\begin{aligned} p(s)&=\frac{\frac{\tau\bar{I}}{A}+\sqrt{\frac{\tau^2\bar{I}^2}{A^2}+4kC\gamma s}}{2k};\\ q(s)&=\frac{\frac{\tau\bar{I}}{A}-\sqrt{\frac{\tau^2\bar{I}^2}{A^2}+4kC\gamma s}}{2k} \end{aligned} \tag{17}$$

$$E_L(s)=(M_LC_L+M_cC_c)s+(\tau+\alpha_L)\bar{I} \tag{18}$$

$$E_H(s)=(M_FC_F+M_HC_H)s+hA_F-(\tau+\alpha_H)\bar{I} \tag{19}$$

$$\beta=\frac{2\rho\bar{I}}{A^2}-\frac{\tau(\bar{T}_H-\bar{T}_L)}{AL} \tag{20}$$

Eq. (11) indicates that the cold-end temperature of the thermoelectric cooler T_L is affected by the variations of the applied current I, the cooling load Q_L and the ambient temperature T_a. $G_I(s)$, $G_Q(s)$ and $G_a(s)$ are the transfer functions accounting for the system dynamic behavior caused by current, cooling load and ambient temperature variations, respectively.

For a thermoelectric cooler performed at a constant cooling load and a fixed ambient condition, we can focus on the system dynamic model:

$$G_I(s)=\frac{\tilde{T}_L(s)}{\tilde{I}(s)}=\frac{N(s)}{sD(s)} \tag{21}$$

2.4. Model reduction

Eq. (21) shows that the dynamic model of a thermoelectric cooler is an infinite-order system. For simplicity in control system design, a model reduction can be made. In practice, the Thomson effect in a thermoelectric module is small as compared to the Seeback effect. Hence, the following approximations can hold:

$$\alpha_H = \alpha_L = \alpha_{pn}; \qquad p(s) = q(s) = \lambda(s) = \sqrt{\frac{C\gamma s}{k}};$$
$$\sinh(\lambda L) \approx \lambda L; \qquad \cosh(\lambda L) \approx 1 + \frac{\lambda^2 L^2}{2}. \tag{22}$$

We then obtain a reduced model for the thermoelectric cooler:

$$G_I(s) = \frac{\tilde{T}_L(s)}{\tilde{I}(s)} = -K\frac{\frac{s}{z}+1}{\left[\frac{s}{p_1}+1\right]\left[\frac{s}{p_2}+1\right]} \tag{23}$$

where

$$K = \frac{\left\{\begin{array}{c} Ak\alpha_{pn}(\bar{T}_H - \bar{T}_L) + L\alpha_{pn}^2\bar{I}\bar{T}_L\left(\dfrac{\rho L^2 h A_F}{A} + 2\rho Lk\right)\bar{I} \\ + \dfrac{\rho L^2\alpha_{pn}}{A}\bar{I}^2 + L\alpha_{pn}hA_F\bar{T}_L \end{array}\right\}}{AA_Fhk + LhA_F\alpha_{pn}\bar{I} - L\alpha_{pn}^2\bar{I}^2} \tag{24}$$

$$z = \frac{AA_Fhk + LhA_F\alpha_{pn}\bar{I} - L\alpha_{pn}^2\bar{I}^2}{\left\{\begin{array}{c}\left[\dfrac{1}{2}A\alpha_{pn}L^2C\gamma + L\alpha_{pn}(M_FC_F + M_HC_H)\right]\bar{T}_L \\ -\dfrac{\rho L^2}{A}(M_FC_F + M_cC_c)\bar{I}\end{array}\right\}} \tag{25}$$

$$p_{1,2} = a \pm \sqrt{\alpha^2 - b^2} \tag{26}$$

$$a = \frac{\left\{\begin{array}{c} Ak(M_FC_F + M_LC_L + M_cC_c + M_HC_H) \\ +LhA_F(M_LC_L + M_cC_c) + AC\gamma L\left(Ak + \dfrac{1}{2}hA_FL\right) \\ +L\alpha_{pn}(M_FC_F + M_LC_L)\bar{I}\end{array}\right\}}{\left\{\begin{array}{c} AL^2C\gamma(M_FC_F + M_LC_L + M_cC_c + M_HC_H) \\ +2L(M_FC_F + M_HC_H)(M_LC_L + M_cC_c)\end{array}\right\}} \tag{27}$$

$$b = \frac{AA_Fhk + LhA_F\alpha_{pn}\bar{I} - L\alpha_{pn}^2\bar{I}^2}{\left\{\begin{array}{c}\dfrac{1}{2}AL^2C\gamma(M_FC_F + M_LC_L + M_cC_c + M_HC_H) \\ +L(M_FC_F + M_HC_H)(M_LC_L + M_cC_c)\end{array}\right\}} \tag{28}$$

Eqs. (24)–(26) indicate that the parameters in the dynamic model, Eq. (23), k, p_1, p_2 and z, are functions of operating conditions $\bar{I}$, $\bar{T}_L$, $\bar{T}_H$. For a typical thermoelectric cooler with $\rho = 10^{-5}\Omega - \mathrm{m}$, $\gamma = 200\ \mathrm{kg\ m^{-3}}$, $A = 0.00145\ \mathrm{m^2}$ $\alpha_{pn} = 0.02\ \mathrm{V\ K^{-1}}$, $k = 1.5\ \mathrm{W\ m^{-1}\ K^{-1}}$, $h = 10\ \mathrm{W\ m^{-2}\ K^{-1}}$, $L = 0.0025\ \mathrm{m}$, $M_c = M_H = 0.05\ \mathrm{kg}$, $M_L = 0.6\ \mathrm{kg}$, $M_F = 0.4\ \mathrm{kg}$, $C_c = C_H = 500\ \mathrm{J\ kg^{-1}\ K^{-1}}$, $C_L = 400\ \mathrm{J\ kg^{-1}\ K^{-1}}$, $C_F = 850\ \mathrm{J\ kg^{-1}\ K^{-1}}$, $A_F = 0.3\ \mathrm{m^2}$, the frequency response is plotted in Fig. 2 which shows that the reduced model, Eq. (23) is identical with the exact model, Eq. (21). The zero and poles of the dynamic model would vary with the operating points as shown in Fig. 3. The gain K increases with increasing cold-end temperature $\bar{T}_L$ and decreasing current $\bar{I}$. The zero z and the poles p_1, p_2 are however approximately constant, irrespective of the variations of current and temperature.

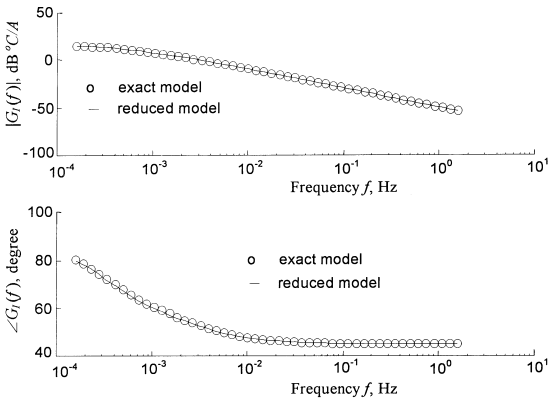

Fig. 2. Exact and reduced model of thermoelectric cooler, $G_I(s)$.

Fig. 2. Modèle exact et réduit du refroidisseur thermoélectrique $G_I(s)$.

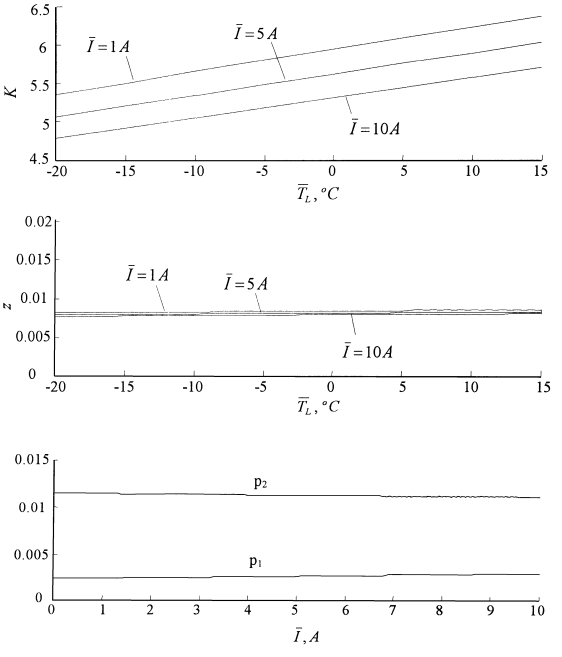

Fig. 3. Variations of gain, zero and poles of the dynamic model $G_I(s)$.

Fig. 3. Variations d'amplification, zéro et pôles du modèle dynamique.

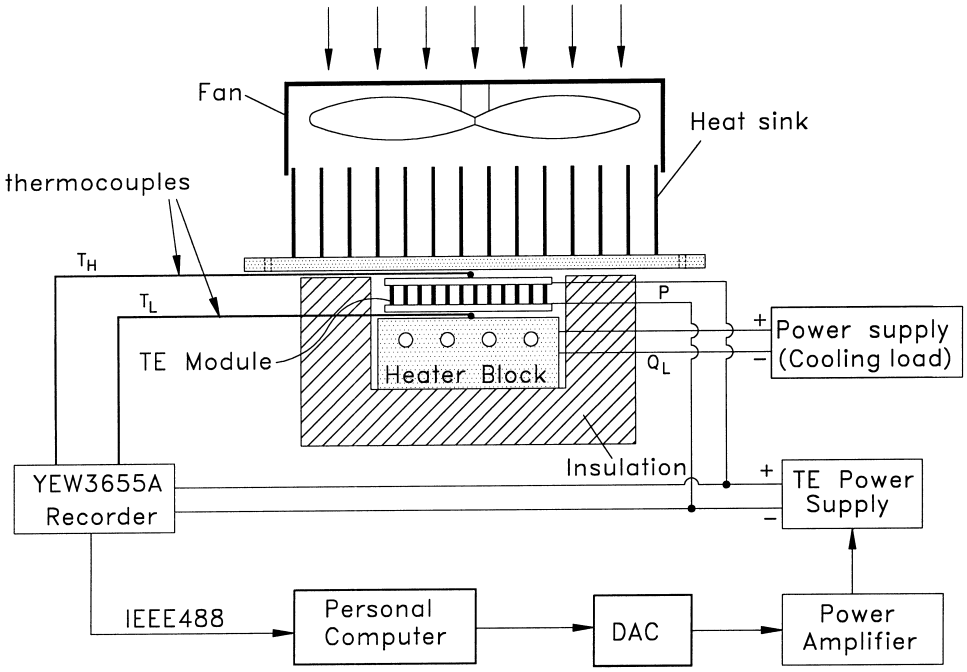

Fig. 4. Facility for system identification of a thermoelectric cooler.

Fig. 4. Facilté d'identification de systèmes d'un refroidisseur thermoélectrique.

2.5. System identification of a thermoelectric cooler

The dynamic model derived theoretically in the present study, Eq. (23), may not be accurate due to many assumptions. Experimental verification is thus required.

Fig. 4 is the schematic diagram of a testing facility for the system dynamic model identification of a thermoelectric cooler. The current of thermoelectric module is regulated by a PC through a DAC (digital-to-analog conversion) device and a DC power amplifier. Three cartridge heaters are embedded in a heater block that is attached to the cold side of the thermoelectric module. The cooling load thus can be emulated by supplying electrical current to the heater. A heat sink is attached to the hot side of the thermoelectric module. A DC fan is installed above the heat sink to blow the heat to the ambient. The heat sink is made from an aluminum finned heat exchangers with 80×80 mm base plate (6 mm thick), 4 mm fin pitch, 26×80 mm fin size (1 mm thick), and 19 fins.

Table 1
Identified parameters at various operating conditions

Tableau 1
Paramètres identifiés pour diverses conditions de fonctionnement

Test no.	$\bar{I}$ (A)	$\tilde{I}$(A)	Q_L (W)	$\bar{T}_L$ (°C)	K	z	p_1	p_2
1	1.5	0.5	0	−6.0	9.5566	0.1375	0.0115	0.5379
2	1.5	0.5	5	2.5	10.1439	0.1360	0.0104	0.5226
3	1.5	0.5	10	11.7	11.0872	0.1421	0.0108	0.5907
4	2.25	0.5	0	−10.1	5.6163	0.1317	0.0135	0.4847
5	2.25	0.5	5	−1.5	6.0544	0.1293	0.0134	0.5018
6	2.25	0.5	10	7.2	7.0804	0.1314	0.0125	0.5500
7	3.0	1.0	0	−14.4	2.3927	0.1319	0.0213	0.6600
8	3.0	1.0	5	−6.8	2.6693	0.1247	0.0197	0.6407
9	3.0	1.0	10	1.6	3.0541	0.1262	0.0193	0.7486
Average value $\bar{K}$, $\bar{z}$, $\bar{p}_1$, $\bar{p}_2$					6.4061	0.1323	0.0147	0.5817

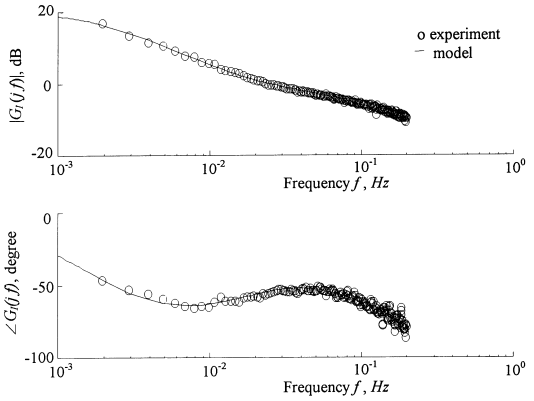

Fig. 5. Comparison of the identified model $G_I(s)$ and the test results.

Fig. 5. Comparaison du modèle identifié $G_I(s)$ et des résultats des essais.

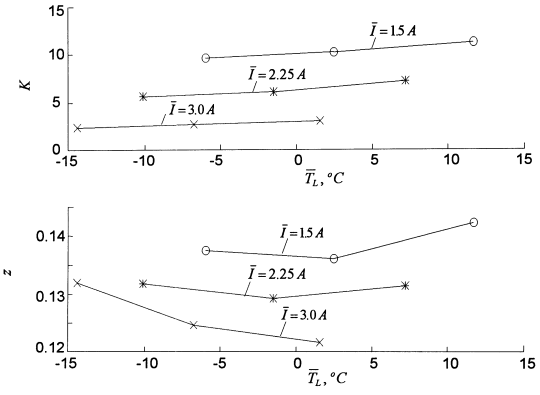

Fig. 7. Variation of the identified parameters K and z with the steady-state cold-end temperature.

Fig. 7. Variation des paramètres identifiés K et z selon la température en régime permanent (côté froid).

A pseudo-random binary sequence (PRBS) voltage generated by using a random number generator in PC is used as the input signal to the thermoelectric module. The clock period of the PRBS signal is 2 s that generates a PRBS signal with 0.2 Hz bandwidth.

All the temperature signals are measured simultaneously by T-type thermocouples and recorded by a 4-channel high speed recorder (Yokogawa YEW3655) with sampling period 0.5 s. A filter with cutoff frequency 50 Hz is used to filter the noises in the signals before recording.

To identify the dynamic model at various operating conditions, we use three steady-state currents (1.5, 2.25, 3.0 A) and three cooling loads (0, 5, 15 W). The steady-state cold-end temperature ranges from −14.4 to 11.7°C.

Table 1 shows the identified parameters at various operating conditions. Fig. 5 is the frequency response of the thermoelectric cooler at $\bar{I} = 1.5\,\text{A}$; $\tilde{I} = 0.5\,\text{A}$; $Q_L = 5\,\text{W}$ and $\bar{T}_L = 25°\text{C}$. The identified model is shown to coincide with the test results very well. Fig. 6 shows the input PRBS signal and the time response of the cold-end temperature.

The variations of the identified parameters with the operating conditions are shown in Figs. 7 and 8. As was predicted qualitatively by the theoretical model, Eq. (23), the gain K increases slightly with increasing cold-end temperature $\bar{T}_L$ but sharply with decreasing current $\bar{I}$. The zero z is approximately constant, irrespective of the change of current and temperature. The poles p_1, p_2 however changes with $\bar{I}$ and Q_L,

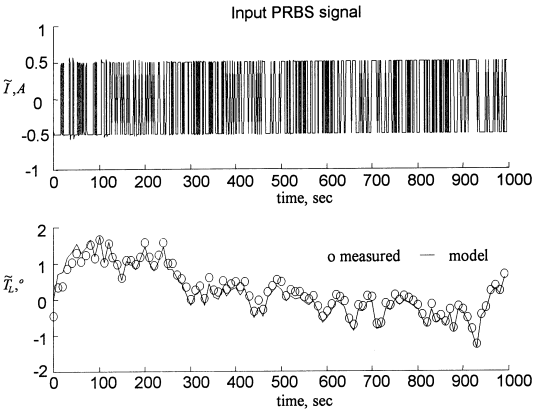

Fig. 6. Input PRBS signal and the temperature response in the system identification.

Fig. 6. Signal PRBS et réponse de la température dans l'identification des systèmes.

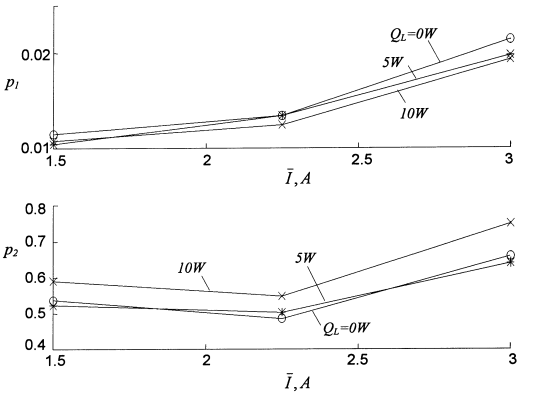

Fig. 8. Variation of the identified parameters p_1 and p_2 with the steady-state current.

Fig. 8. Variation des paramètres identifiés p_1 et p_2 avec l'écoulement en courant en régime permanent (côté froid).

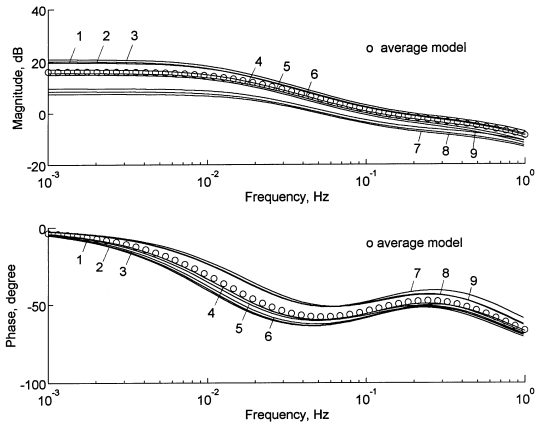

Fig. 9. Identified dynamic model $G_I(s)$ at various operating conditions and the average model.

Fig. 9. Modèle dynamique identifié $G_I(s)$ sous diverses conditions de fonctionnement et le modèle moyen.

qualitatively different from the theoretical model, Eq. (21). This is resulted from the assumptions used in the derivation, especially the assumption of linear temperature distribution at steady state in the thermoelectric legs.

2.6. Synthesis of the nonlinear dynamic model of a thermoelectric cooler and the average model

The variation of the identified parameters with the steady-state operating point reveals that the dynamic model of a thermoelectric cooler is basically nonlinear. The actual nonlinear model can be treated as the synthesis of several linearly-perturbed models identified at various operating points.

For easy implementation in controller design, an average model is defined using the average parameters $\bar{K} = 6.4061$, $\bar{z} = 0.1323$, $\bar{p}_1 = 0.0147$, $\bar{p}_2 = 0.5817$. The identified linear-perturbation models and the average model are presented in Fig. 9. The average model will be used in the controller design.

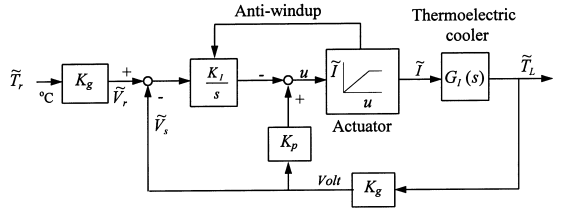

Fig. 10. Linear feedback control system structure.

Fig. 10. Rétroaction linéaire et structure du système de régulation.

3. Temperature control of a thermoelectric cooler

3.1. Controller design

Using the above average dynamic model of the thermoelectric cooler, we design a controller for the cold-end temperature control. We use a controller structure similar to PI feedback as shown in Fig. 10 with an anti-windup design. This controller belongs to the pseudo derivative feedback (PDF) structure [9,10] but without derivative terms.

Using the average model, we obtain a closed-loop transfer function:

$$\frac{\tilde{T}_L(s)}{\tilde{T}_r(s)} = \frac{K_I K_g A_p \bar{K}\left(\dfrac{s}{\bar{z}_1}+1\right)}{\left\{\begin{array}{c}\dfrac{1}{\bar{p}_1\bar{p}_2}s^3+\left(\dfrac{1}{\bar{p}_1}+\dfrac{1}{\bar{p}_2}+\dfrac{K_g A_p \bar{K}}{\bar{z}}K_p\right)s^2 \\ +\left(1+\dfrac{K_g A_p \bar{K}}{\bar{z}}K_I+K_g A_p \bar{K} K_p\right)s \\ +K_I K_g A_p \bar{K}\end{array}\right\}}, \quad (29)$$

where A_p is the proportional constant of the actuator. It is seen that for the PDF controller structure, we can easily place the closed-loop poles by adjusting the controller parameters K_I and K_p. By computer simulation and assuming that the feedback system is at critical damping condition ($\zeta = 1$) with equal closed-loop poles, we found that $K_I = 73$ and $K_p = 227$ will give a response without overshoot.

The feedback system exhibits a good performance with respect to the variation of plant dynamics. For example, if the plant (thermoelectric cooler) gain K varies from 1 to 20 (but with poles and zero fixed at the

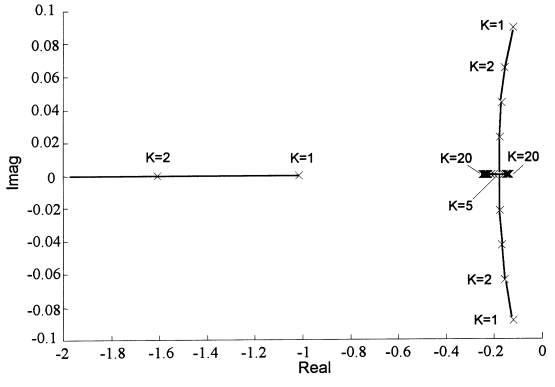

Fig. 11. Root locus of the closed-loop system for the variation of plant gain K at fixed $\bar{p}_1$, $\bar{p}_2$, $\bar{z}$.

Fig. 11. Emplacement de la racine du système à boucle fermée selon les variations en termes d'amplification de l'installation K dans les conditions déterminées $\bar{p}_1$, $\bar{p}_2$, $\bar{z}$.

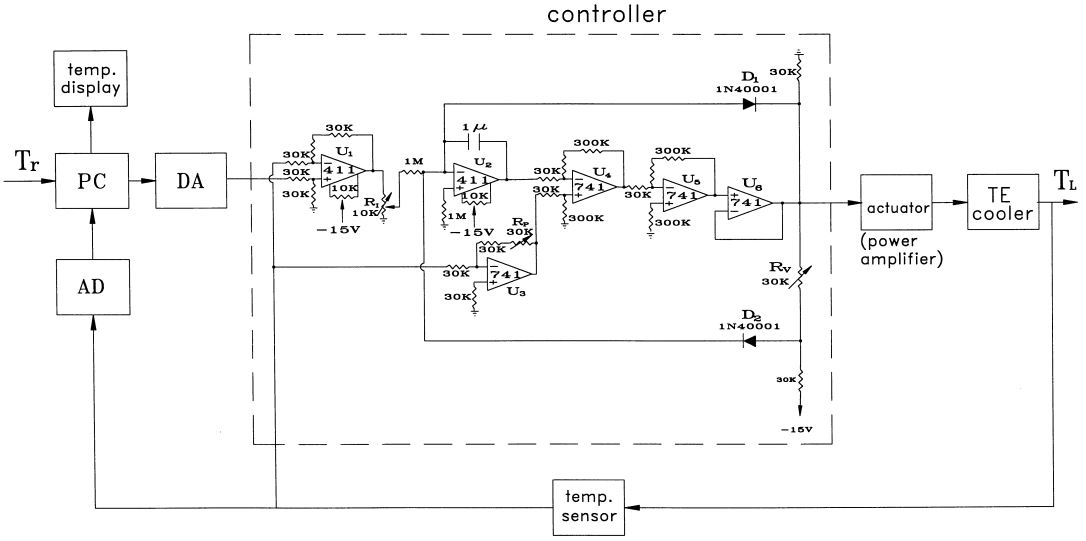

Fig. 12. Analog control system design.

Fig. 12. Conception du système de régulation analogique.

average values $\bar{p}_1$, $\bar{p}_2$, $\bar{z}$), the root locus of the closed-loop system for varying K is still on the left s-plane as shown in Fig. 11. The breakaway point is around $K = 5$ which is very close to the average model $K = 6.4061$. The feedback system performance is thus expected to be satisfactory even under the variations of plant dynamics. This resistance to the variation of plant dynamics is quite important for a controller design.

3.2. Controller implementation and test results

To implement the control system for the temperature control of a thermoelectric cooler, we design an analog circuit as shown in Fig. 12 according to the control system structure (Fig. 10). For easy implementation, a personal computer is used for the measurement and display of the system response, for giving a command of temperature setting value, and for outputting an analog control signal (4–20 mA) through a DA interface.

We performed two kinds of tests, namely, temperature regulation and disturbance-rejection capability, to evaluate the controller design. Fig. 13 shows that the simulation of the cold-end temperature T_L response for a step setting agrees very well with the experimental

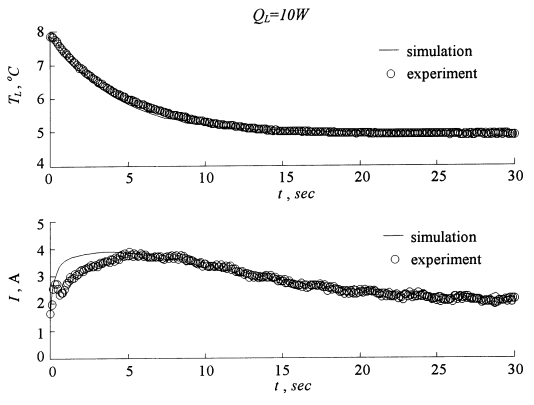

Fig. 13. Time response of cold-end temperature T_L and control signal variation I for a step setting at $Q_L = 10$ W.

Fig. 13. Réponse au niveau de la température du côté froid en fonction de la durée T_L et régulation de la variation du signal I lors de régulation par paliers à $Q_L = 10$ W.

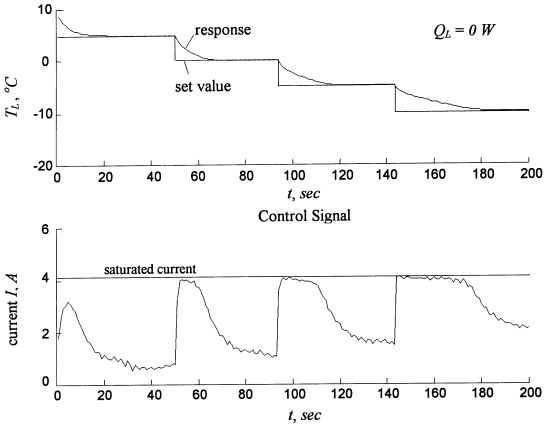

Fig. 14. Time response of cold-end temperature T_L and control signal variation I for consequent step settings at $Q_L = 0$ W.

Fig. 14. Réponse au niveau de la température du côté froid en fonction de la durée T_L et régulation de la variation du signal I lors des régulation par paliers suivantes à $Q_L = 0$ W.

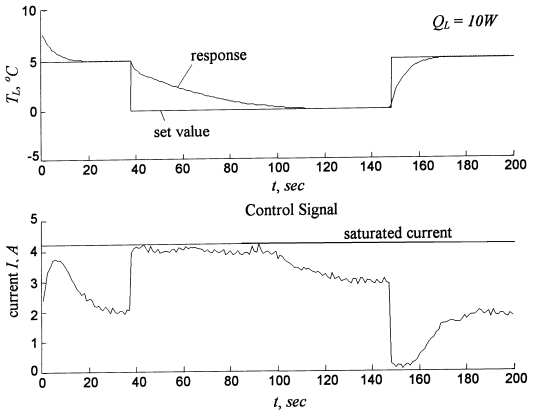

Fig. 15. Time response of cold-end temperature T_L and control signal variation I for consequent step settings at $Q_L = 0$ W.

Fig. 15. Réponse au niveau de la température du côté froid en fonction de la durée T_L et régulation de la variation du signal I lors des régulation par paliers suivantes à $Q_L = 0$ W.

results. A slight deviation in the control signal (current I) at the beginning is probably due to the thermal inertia of the cold-end heat exchanger and the heat sink. The thermal mass absorbs a relatively large amount of heat at the transient period and causes an additional heat pumping effect. The current is thus slightly lowered.

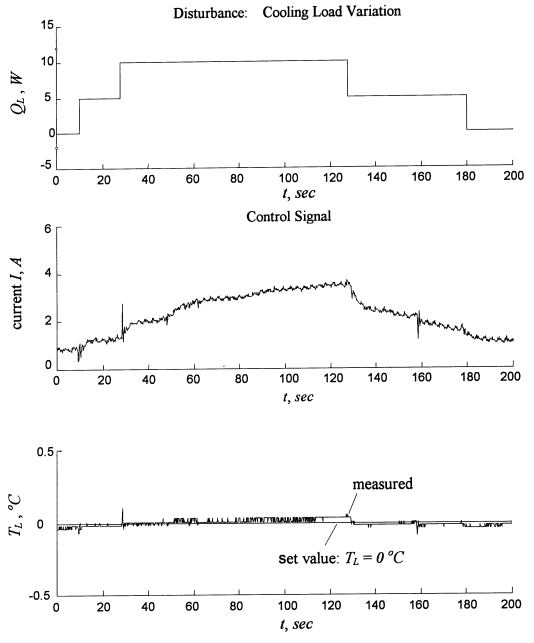

Fig. 16. Disturbance-rejection capability tests for a fixed setting $T_L = 0$°C.

Fig. 16. Essais sur la capacité de perturbation/rejet pour une régulation fixe de $T_L = 0$°C.

Fig. 14 shows the temperature responses for the set value of 10°C→5°C→0°C→−5°C→−10°C at $Q_L = 0$ W. The steady-state errors are very small. The response time is around 20 s for T_L changing from 5 to 0°C. However, the response time gets longer for lower setting temperature. It takes about 35 s for T_L changing from −5 to −10°C and a longer saturation time for the control signal (current) occurs.

Tests are also conducted at higher cooling load, i.e. $Q_L = 10$ W. The temperature set values are from 5 to 0°C, then back to 5°C. Fig. 15 shows that no steady-state error was observed. The response time for step-down setting to 0°C is around 70 s. However, it takes only about 20 s for step-up setting from 0°C. The longer response time for the step-down setting is due to the control signal (current) saturation which occurs for a longer time duration as shown in Fig. 15. For step-up setting, the cold end can be easily warmed up by the heat conduction loss of the thermoelectric module from the hot to the cold end. In this case, no control signal saturation is observed.

The disturbance-rejection capability is a very important property of the control system. The tests are conducted at a fixed set temperature ($T_r = 0$°C) under a varying cooling load from 0 W→5 W→10 W→5 W→0 W as shown in Fig. 16. The control signal and the temperature response are shown in Fig. 16. It is seen that T_L is maintained at a fixed value (0°C) within ±0.1°C irrespective of the cooling load variation. Some other tests are also conducted with a fast air temperature variation for the heat sink (by moving a hot air blower back and forth on the top of the heat sink). This test corresponds to an environmental test. A very good temperature control is obtained too. This indicates that the present control system has a good performance with respect to the disturbance rejection.

4. Discussion and conclusion

The controller design for temperature control of a thermoelectric cooler is not very simple due to the nonlinear dynamic behavior of the thermoelectric module. The effect of dynamic behavior of the thermal masses of the heat sink and the cooling-load heat exchanger imposes another problem on the control system design. In the present study, we derived a linear dynamic model for the whole thermoelectric cooler using small-signal linearization method. It shows that the structure of the dynamic model of a thermoelectric cooler has two poles and one zero. The linear dynamic model is shown to vary with operating conditions. The actual nonlinear dynamic model of a thermoelectric cooler can be treated as the synthesis of the linear-perturbation models at various operating conditions.

For a controller design using linear feedback theory, we adopt an average linear dynamic model for the

thermoelectric cooler. A linear feedback system similar to PDF structure is designed for the cold-end temperature control of a thermoelectric cooler. The controller parameters are tuned by computer simulation for the feedback system at critical damping condition and without overshoot.

To verify the feasibility of the linear feedback system design using the average linear dynamic model of the plant for the control of a nonlinear system, we designed and fabricated an analog control system to control the cold-end temperature of a thermoelectric cooler. Step response tests show that the temperature regulation is very satisfactory with small steady-state error. The response time, however, changes with the direction of step change, the cold-end temperature, and the magnitude of the cooling load. Step-down setting has a slower response than the step-up setting. Smaller cooling load causes faster response. Lower cold-end temperature has a slower response.

As to the disturbance-rejection property of the controller, we performed some severe tests under fast variations of cooling load and ambient temperature. Experimental results show that T_L can be maintained at the fixed value within ± 0.1°C irrespective of the variations of the cooling load and the ambient conditions. This also indicates that the present PDF controller using the average model has a good performance in disturbance rejection.

Acknowledgements

The present study was supported by the National Science Council, Taiwan, ROC, through Grant No. NSC83-0413-E002-001.

References

[1] Goldsmid H. J Electronic Refrigeration. Englewood Cliffs (NJ): Prentice-Hall, Inc, 1986. (chapter 8).
[2] Marlow R, Buist RJ, Nelson JL. System aspects of thermoelectric coolers for hand held thermal viewers. Fourth international conference on thermoelectric energy conversion, 1982, IEEE Catalog No. 82CH1763-2. p. 125–9.
[3] Andersen JR. Thermoelectric air conditioner for submarines. Adv Energy Conv 1962;2:241–8.
[4] Gray PE. The dynamic behavior of thermoelectric devices. New York and London: John Wiley and Sons, Inc, 1960.
[5] Stoecker WF, Chaddock JB. Transient performance of a thermoelectric refrigerator under step-current control. ASHARE 1963;5:61–7.
[6] Bywaters RP, Blum HA. The transient behavior of cascade thermoelectric heat pumps. Energy Conversion 1970;10:193–200.
[7] Hoyos GE, Rao KR, Jerger D. Numerical analysis of transient behavior of thermoelectric cooler. Energy Conversion 1977;17:23–9.
[8] Soo SL. Direct energy conversion. Englewood Cliffs (NJ): Prentice-Hall Inc., 1968 (chapter 5).
[9] Phelan RM. Feedback control system. Cornel University, Itheca (NY): Sibley School of Mechanical and Aeronautical Engineering, (privately published notes),
[10] Leu MC. PDF subvariable control and its application to robot motion control. ASME Journal of Dynamic System, Measurement, and Control. 1989; 452–61.